 

# Self-Consistent Cluster Approximation Analysis of the OH Stretching Bands of Methanol in the Liquid State

**Isao Kanesaka**†

Faculty of Science, Toyama University, 3190 Gofuku, Toyama 930-8555

Received September 24, 2008; E-mail: kanesaka@po6.nsk.ne.jp

The isotropic and anisotropic Raman spectra and the infrared spectrum of O–H stretching bands of $CH_3OH$ in the liquid state are analyzed on the basis of a self-consistent cluster theory based on Green's function. The observed spectra are explained well in terms of three clusters constructed by combining two intrinsic modes. The probability of the higher and lower intrinsic modes is 0.28 and 0.72, respectively. Two intrinsic modes derived are 3425.5 and 3320.1 $cm^{-1}$, where the former is recognized for the first time, and they are assigned to a H-bonded OH stretching perturbed by an OH stretching in the other chain or a Y junction and that remains unperturbed, respectively. A weak band at 3529.2 $cm^{-1}$ found also for the first time is assigned to a local mode in a chain end. Overtones of the OH stretching are satisfactorily explained by fundamentals derived here. The molecules in a chain are evaluated to be 17 with mainly a tetrahedral configuration about the H-bond. In a symmetric cluster a line shape of component bands is asymmetric and their peak positions and bandwidths are discussed with a boundary parameter.

In a liquid state, a vibrational linear coupling between two oscillators through an oscillating dipole–dipole interaction results in differences in peak positions and bandwidths among infrared, isotropic and anisotropic Raman spectra. We have analyzed vibrational spectra of some systems by use of a vibrational coupling model.[1–4] In the case of C=O stretching bands of acetone,[4] the three types of spectra are explained in terms of a strong orientational correlation between two like oscillators. In the present study we are interested in O–H stretching bands of $CH_3OH$, which reflect strongly H-bonded structures. Some attempts[5–8] have been carried out to analyze the three types of spectra of the O–H stretching bands of methanol. Maillard et al.[5] have explained them in terms of a cyclic structure of polymers with an average degree of polymerization of 5–6. On the other hand, Torii et al.[6–8] have analyzed the spectra on the basis of a chain structure derived from a molecular dynamics simulation. Since many experimantal[9–12] and numerical[13–21] investigations have deduced the chain like structure of methanol, although Pieruccini[22] has supported the cyclic structure of ca. 6 molecules, Torii's analysis[6–8] may be plausible, although his explanation is qualitative. Our method used previously may be useful, as shown for some systems.[1–4] However, the method may be insufficient for the present system consisting of disordered chains, because a vibrational coupling between two oscillators is only considered, ignoring couplings with the other part of a chain.

In the present study we will analyze the infrared and Raman spectra of the O–H stretching bands of $CH_3OH$ on the basis of the Green's function. That is a cluster approximation called the self-consistent boundary site (SCBS) approximation developed by Butler.[23] The SCBS approximation which is developed to obtain the density of state of disordered alloys treats a local cluster of atoms exactly and the more removed regions of the system in an approximate but self-consistent fashion. In the present study disordered chains consisting of O–H oscillators are divided into three clusters, which are constructed by combining two intrinsic modes. The remaining parts of the Hamiltonian consist of averaged quantities, that is so-called a medium with a coherent potential. The analytical procedure of the SCBS approximation will be given in detail and the adequacy of its application to the present system is discussed in relation to the liquid structure.

Many workers[5–8,24–40] have investigated the infrared and Raman spectra of the O–H stretching bands of methanol in relation to intermolecular interactions and liquid structures. A broad infrared band at 3340 $cm^{-1}$ is approximately fitted with one Gaussian function and is believed to contain contributions from various H-bonded aggregates present.[36,39] Bourderon et al.[27,28] have observed four bands in the first overtone of the OH stretching, demonstrating the presence of oligomers and monomers. Many investigations of oligomers have been carried out for dilute solutions of $CCl_4$, clarifying five bands, which are explained in terms of monomer, open dimer, cyclic trimer, and cyclic tetramer.[37] In the Raman spectra two bands, one polarized, the other depolarized, are observed and explained in terms of two modes in a quasicrystalline structure of liquid methanol.[29–31] The structures of liquid methanol have been investigated experimetally[5–12] and numerically,[13–21] deducing an ensemble of chain aggregates of various sizes, including occasional Y junctions. The theoretical analysis of the infrared and Raman spectra of the OH stretching bands has been done by Maillard et al.[5] and Torii et al.,[6–8] as described above.

## Experimental

Anhydrous $CH_3OH$ obtained commercially was used without further purification. The Raman spectra were recorded with a

† Present address: Meirin-cho 1-242 717, Toyama 930-0001

Published on the web August 7, 2009; doi:10.1246/bcsj.82.946

JASCO NR-1100 Raman spectrometer using laser excitation at 514.5 nm and 200 mW. The polarized and depolarized Raman spectra, $I_{pol}(\nu)$ and $I_{dep}(\nu)$, were observed operating an incident light with a $1/2\lambda$ plate without a polarizer in a scattered light. The scattered conditions in the Porto's notation are: $[X(Z,Z)Y]$ and $[X(Z,X)Y]$ for $I_{pol}(\nu)$ and $[X(Y,X)Y]$ and $[X(Y,Z)Y]$ for $I_{dep}(\nu)$. The infrared spectra were measured with a JASCO IR-810 spectrometer, putting the sample between the KRS-5 plates. The observed infrared and Raman wavenumbers were calibrated using those of polystyrene and mercury lines, respectively. They are believed to be accurate to within $\pm 2\,cm^{-1}$. The isotropic Raman spectrum was obtained as[41]

$$I_{iso}(\nu) = I_{pol}(\nu) - \frac{7}{6} I_{dep}(\nu) \tag{1}$$

**SCBS Approximation.**[23] As realized later, the intrinsic modes of the O–H stretchings are at least two, whose wavenumbers are denoted as $\nu_1$ and $\nu_2$ ($\nu_1 > \nu_2$). Hence, in the cluster approximation, there needs to be three clusters, $\mathbf{G_1}$, $\mathbf{G_2}$, and $\mathbf{G_3}$, which consist of two $\nu_1$ sites, two $\nu_2$ sites, and $\nu_1$ and $\nu_2$ sites, respectively, and their probability is given by $n_1^2$, $(1-n_1)^2$, and $2n_1(1-n_1)$, which are denoted as $P_1$, $P_2$, and $P_3$; $n_1$ is the probability of the $\nu_1$ site. The remaining parts of the Hamiltonian, that is the medium, are given by the coherent potential and the coupling constant, which fulfill self-consistent relations with three clusters. In a linear chain system assumed here, the Hamiltonian with the cluster, for example, of $\varepsilon_1$ and $\varepsilon_2$ is given as

$$\tilde{H} = \begin{vmatrix} \ddots & & & & & & \\ & \sigma & W_0 & & & & 0 \\ & W_0 & \sigma & W_0 & & & \\ & & W_0 & \varepsilon_1 & W_3 & & \\ & & & W_3 & \varepsilon_2 & W_0 & \\ & & & & W_0 & \sigma & W_0 \\ & 0 & & & & W_0 & \sigma \\ & & & & & & \ddots \end{vmatrix} \tag{2}$$

where $\sigma$ is the coherent potential and $W_0$ the averaged coupling constant. The Green's function of $\mathbf{G_3}$ is given as

$$\mathbf{G_3}(\nu) = \begin{vmatrix} {\nu_1}^2 - \nu^2 + i\nu\Gamma_1 - \nu A(\nu) & \nu f_3 \\ \nu f_3 & {\nu_2}^2 - \nu^2 + i\nu\Gamma_2 - \nu A(\nu) \end{vmatrix}^{-1} \tag{3}$$

where the following relations are used because of the vibrational Green's function:[42]

$$\varepsilon_i = {\nu_i}^2 - \nu^2 + i\nu\Gamma_i \tag{4}$$

and

$$W_3 = \nu f_3 = \nu({f_3}^r + i{f_3}^i) \tag{5}$$

where $\nu_i$ is defined above, $\Gamma_i$ is the damping constant and ${f_3}^r$ and ${f_3}^i$ are the mechanical and damping coupling constants, respectively. $\nu A(\nu)$ is the boundary parameter, which gives the contribution from the nearest neighbor medium site, and, hence, given as

$$\nu A(\nu) = \frac{{W_0}^2}{\sigma - \nu A(\nu)} \tag{6}$$

$W_0$ is given as

$$W_0 = \nu f = \sum_{i=1,3} P_i \nu f_i \tag{7}$$

It should be noted that $\nu A(\nu)$ in the denominator in eq 6 comes from the second nearest neighbor medium site and so on, resulting in a ladder function. The Green's functions of $\mathbf{G_1}$ and $\mathbf{G_2}$ with $\varepsilon_1 = \varepsilon_2 = {\nu_1}^2 - \nu^2 + i\nu\Gamma_1$ and $\varepsilon_1 = \varepsilon_2 = {\nu_2}^2 - \nu^2 + i\nu\Gamma_2$, respectively, are also defined. Hence, the total Green's function consisting of three clusters is given as

$$\begin{aligned} \mathbf{G}(\nu) &= \sum_{i=1,3} P_i \mathbf{G_i}(\nu) \\ &= \sum_{i=1,2} P_i \begin{vmatrix} {\nu_i}^2 - \nu^2 + i\nu\Gamma_i - \nu A(\nu) & \nu f_i \\ \nu f_i & {\nu_i}^2 - \nu^2 + i\nu\Gamma_i - \nu A(\nu) \end{vmatrix}^{-1} \\ &\quad + P_3 \begin{vmatrix} {\nu_1}^2 - \nu^2 + i\nu\Gamma_1 - \nu A(\nu) & \nu f_3 \\ \nu f_3 & {\nu_2}^2 - \nu^2 + i\nu\Gamma_2 - \nu A(\nu) \end{vmatrix}^{-1} \end{aligned} \tag{8}$$

The diagonal element of the medium, $\bar{\mathbf{G}}_{\mathbf{00}}$, is given as

$$\bar{\mathbf{G}}_{\mathbf{00}} = \frac{1}{\sigma - 2\nu A(\nu)} = \left( \frac{\nu^2 f^2}{\nu A(\nu)} - \nu A(\nu) \right)^{-1} \tag{9}$$

where eq 6 is used for the last formulae. In the SCBS approximation the self-consistent condition is taken using the boundary site of $\mathbf{G}(\nu)$, the 1,1 element of $\mathbf{G}(\nu)$, as

$$\mathbf{G_{11}}(\nu) = \bar{\mathbf{G}}_{\mathbf{00}}(\nu) \tag{10}$$

In the present analysis $A(\nu)$ is determined using eq 10 by the least-squares method.

The infrared spectrum is calculated as[4]

$$\begin{aligned} I(\nu) &= -\nu \mathrm{Im} \left| \sum_{i=1,2} P_i \tilde{\mathbf{T}}_i \mathbf{G_i}(\nu) \mathbf{T}_i + P_3 \tilde{\mathbf{T}}_3 \mathbf{G_3}(\nu) \mathbf{T}_3 \right| \\ &= -\nu \mathrm{Im} \left| \sum_{i=1,2} P_i \tilde{\mathbf{T}}_i \mathbf{L} \tilde{\mathbf{L}} \mathbf{G_i}(\nu) \mathbf{L} \tilde{\mathbf{L}} \mathbf{T}_i + P_3 \tilde{\mathbf{T}}_3 \mathbf{G_3}(\nu) \mathbf{T}_3 \right| \\ &= -\nu \mathrm{Im} \sum_{i=1,2} P_i \tilde{\mathbf{T}}_i \mathbf{L} \begin{vmatrix} g_s(\nu) & 0 \\ 0 & g_{as}(\nu) \end{vmatrix}_i \begin{vmatrix} \frac{1}{\sqrt{2}}(\boldsymbol{\mu}_1 + \boldsymbol{\mu}_2) \\ \frac{1}{\sqrt{2}}(\boldsymbol{\mu}_1 - \boldsymbol{\mu}_2) \end{vmatrix}_i \\ &\quad - \nu \mathrm{Im} P_3 \tilde{\mathbf{T}}_3 \mathbf{G_3}(\nu) \mathbf{T}_3 \end{aligned} \tag{11}$$

where $\mathbf{L}$ is the eigen vector of $\mathbf{G_1}(\nu)$ and $\mathbf{G_2}(\nu)$ and given as

$$\mathbf{L} = \begin{vmatrix} \frac{1}{\sqrt{2}} & \frac{1}{\sqrt{2}} \\ \frac{1}{\sqrt{2}} & -\frac{1}{\sqrt{2}} \end{vmatrix} \tag{12}$$

$\mathbf{T}$ is the intensity parameter matrix given, for example, as $\tilde{\mathbf{T}}_3 = |\boldsymbol{\mu}_1 \quad \boldsymbol{\mu}_2|$, where $\boldsymbol{\mu}_1$ and $\boldsymbol{\mu}_2$ correspond to the transition moment of the $\nu_1$ and $\nu_2$ sites, respectively. Although the infrared spectrum for $\mathbf{G_1}(\nu)$ or $\mathbf{G_2}(\nu)$ is hence obtained by the same manner as that for the C=O stretching bands of acetone,[4] the last term in eq 11 is analyzed without diagonalization, because the eigen vector of $\mathbf{G_3}(\nu)$ is generally complex; a line shape similar to $\mathbf{G_3}(\nu)$ is discussed in our recent study.[43] The Raman spectra are calculated removing the factor $\nu$ from eq 11 and using the Raman tensor, $\boldsymbol{\alpha}_i$, for $\boldsymbol{\mu}_i$.[4,44–47] In eq 11 $g_s(\nu)$ and $g_{as}(\nu)$ are the shape function of the symmetric and asymmetric modes, respectively, and both components are observed in the infrared and depolarized Raman spectra, whereas $g_s(\nu)$ is only observed in the isotropic Raman spectrum. On the other hand, the two component bands of $\mathbf{G_3}(\nu)$, $\nu_+$ and $\nu_-$, are observed in the three types of spectra; $\nu_+ > \nu_1$ and $\nu_- < \nu_2$.

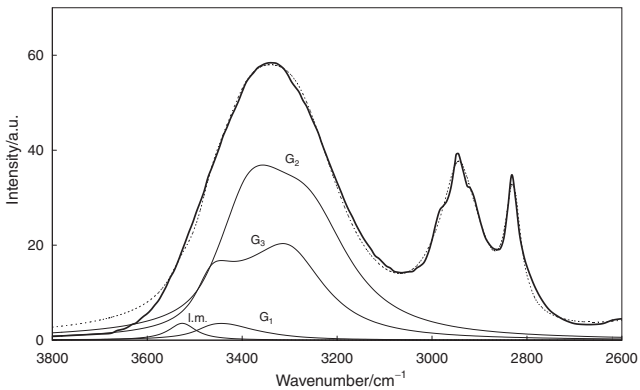


**Figure 1.** The observed (broad solid line) and simulated (dotted line) infrared spectra of the OH stretching bands of $CH_3OH$. The bands due to the clusters and the local mode are given by the thin solid line. The bands other than the OH stretchings are omitted.

The infrared band other than the O–H stretchings is analyzed as

$$I_k(\nu) = -\nu \mathrm{Im} \frac{{t_k}^2}{{\nu_k}^2 - \nu^2 + i\nu\Gamma_k} \tag{13}$$

where $t_k$ is the intensity factor (scalar) of the $k$-th band. The Raman band is analyzed similarly by removing the factor $\nu$ from eq 13.

## Results and Discussion

The observed infrared spectrum is given by the broad solid line in Figure 1 and the observed isotropic and anisotropic Raman spectra in Figures 2a and 2b, respectively. The isotropic Raman spectrum consists of the main band at 3280 cm$^{-1}$ and the broad shoulder at ca. 3450 cm$^{-1}$. On the other hand, only a broad band is observed at 3366 or 3340 cm$^{-1}$ in the anisotropic or infrared spectrum, respectively. From the isotropic and anisotropic Raman bands one of the intrinsic modes is expected to be their intermediate, that is $\nu_2 \approx 3325\,\mathrm{cm}^{-1}$. The shoulder isotropic Raman band may be due to $\nu_1$, although it is not clear whether $\nu_1$ is higher than the shoulder band or not. It is certain that $\nu_2$ is assigned to the fully H-bonded OH stretching, whereas the origin of $\nu_1$ is obscure, which is discussed later.

The total Green's function, $\mathbf{G}(\nu)$ in eq 8, relates to the density of state, which should be unique. This means that the parameters in $\mathbf{G_1}$, $\mathbf{G_2}$, and $\mathbf{G_3}$ should be common in the three types of spectra. On the other hand, it is impossible to analyze simultaneously the three types of spectra in the present stage by the least-squares method, resulting in variation of parameters. The small variation is obtained in the case of $n_1 = 0.28$, giving rise to $P_1 = 0.08$, $P_2 = 0.52$, and $P_3 = 0.40$, indicating predominance of $\mathbf{G_2}$ and $\mathbf{G_3}$.

The simulated spectra and the cluster's bands are given by the broken and thin solid lines in Figures 1 and 2, respectively, where the bands other than the O–H stretching are not given. In the course of the analysis it was found that there is a weak band at 3529.2 cm$^{-1}$, which is treated as an isolated band and noted as l.m. (local mode) in Figures 1 and 2. The agreement between the observed and simulated spectra is good, as seen in Figures 1 and 2, although less agreement is seen in regions higher than 3600 cm$^{-1}$ in Figure 1, which results mainly from the Green's function based on the Lorentzian-like band. As

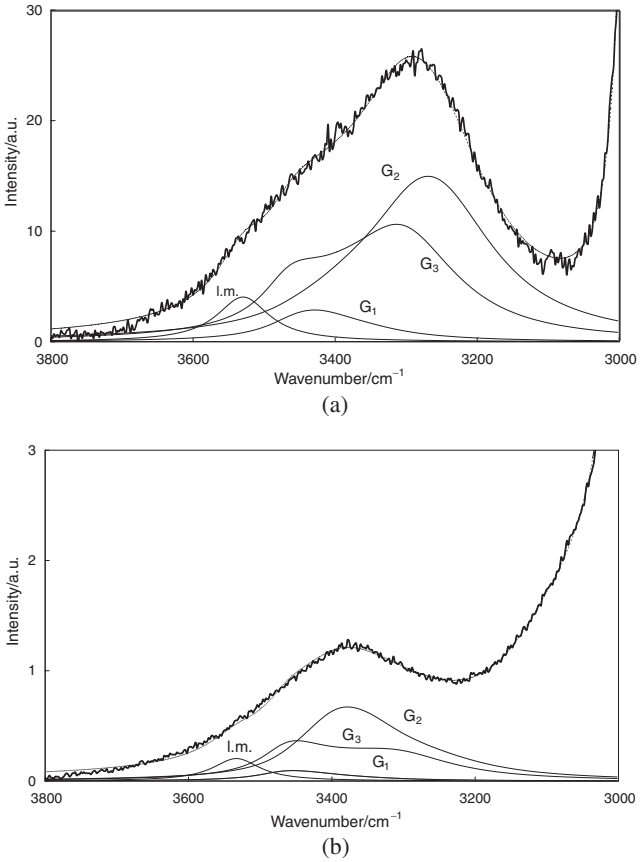


**Figure 2.** (a) The observed (broad solid line) and simulated (dotted line) isotropic Raman spectra of the OH stretching bands of $CH_3OH$. (b) The observed (broad solid line) and simulated (dotted line) anisotropic Raman spectra of the OH stretching bands of $CH_3OH$. The other captions are the same as those in Figure 1.

seen in Figure 2a, the main isotropic Raman band at 3280 cm$^{-1}$ is explained in terms of $g_s(\nu)$ in $\mathbf{G_2}$ and $\nu_-$ in $\mathbf{G_3}$. The shoulder band at ca. 3450 cm$^{-1}$ is assigned to $g_s(\nu)$ in $\mathbf{G_1}$ and $\nu_+$ in $\mathbf{G_3}$, where the latter is predominant. In the depolarized Raman spectrum the main band at 3366 cm$^{-1}$ is assigned to $g_{as}(\nu)$ in $\mathbf{G_2}$. Although the intensity due to $\mathbf{G_3}$ is considerably large, $\nu_+$ and $\nu_-$ do not give clear structures or shoulders in the depolarized spectrum. The main infrared band at 3340 cm$^{-1}$ is assigned both to $g_{as}(\nu)$ and $g_s(\nu)$ in $\mathbf{G_2}$ and $\nu_-$ in $\mathbf{G_3}$. In $\mathbf{G_1}$ and $\mathbf{G_2}$ the infrared intensity ratio of $g_s$ and $g_{as}$ is given as $I_s/I_{as} = (1 + \cos\theta)/(1 - \cos\theta)$, where $\theta$ is the orientational angle between two oscillators. From $\theta_2 = 70.7°$ $I_s$ is larger than $I_{as}$, although the inverse relation is seen in Figure 1. This results from $f_2^i$, which makes $g_s(\nu)$ broad and $g_{as}(\nu)$ sharp. The ratio $|\boldsymbol{\mu}_1|/|\boldsymbol{\mu}_2|$ derived is 0.72. The values of the Raman tensor defined in the bond fixed coordinate system ($z \parallel$ bond axis) in arbitrary unit are: $\alpha_{xx} = 2.2$, $\alpha_{yy} = 2.2$, $\alpha_{zz} = 1.3$ and $\alpha_{xx} = 2.3$, $\alpha_{yy} = 2.4$, $\alpha_{zz} = 1.3$ for the $\nu_1$ and $\nu_2$ sites, respectively, and the degree of depolarization is 0.014 and 0.021. The band constants, $\nu_i$ and $\Gamma_i$, and the coupling constants, $f^r$ and $f^i$, are summarized in Table 1, where the orientational angle between two oscillators in $\mathbf{G_i}$, $\theta_i$, is also given for the infrared and depolarized Raman spectra; the

**Table 1.** The Band Constants, $\nu_i$ and $\Gamma_i$, and the Coupling Constants, $f^r$ and $f^i$, in $cm^{-1}$ in the O–H Stretching Bands of $CH_3OH$

| | | $\nu_i$ | $\Gamma_i$ | $f^r$ | $f^i$ | $\theta$ /degree |
|---|---|---|---|---|---|---|
| IR | $\mathbf{G_1}$ | 3425.5 | 112.1 | −35.8 | 10.7 | 56.6 |
| | $\mathbf{G_2}$ | 3316.6 | 153.1 | −96.2 | 46.7 | 70.7 |
| | $\mathbf{G_3}$[a)] | — | — | −65.5 | 23.3 | 73.2 |
| Iso | $\mathbf{G_1}$ | 3425.1 | 119.8 | −35.2 | 10.4 | |
| | $\mathbf{G_2}$ | 3321.2 | 150.3 | −95.7 | 40.2 | |
| | $\mathbf{G_3}$[a)] | — | — | −63.2 | 20.1 | |
| Dep | $\mathbf{G_1}$ | 3425.9 | 120.2 | −35.8 | 11.0 | 55.8 |
| | $\mathbf{G_2}$ | 3322.5 | 156.1 | −90.5 | 45.4 | 72.2 |
| | $\mathbf{G_3}$[a)] | — | — | −60.2 | 20.4 | 70.8 |
| Averaged | $\mathbf{G_1}$ | 3425.5 | 117.4 | −35.6 | 10.7 | 56.2 |
| | $\mathbf{G_2}$ | 3320.1 | 153.2 | −94.1 | 44.1 | 71.5 |
| | $\mathbf{G_3}$[a)] | — | — | −63.0 | 21.3 | 72.0 |

a) The band constants in $\mathbf{G_3}$ are the same as those in $\mathbf{G_1}$ and $\mathbf{G_2}$.

isotropic Raman spectrum does not depend on $\theta$, because $f$, which depends implicitly on $\theta$ in the present analysis, is treated as the independent parameter, by also inferring that the trace of $\alpha_i$ does not depend on the transformation from the bond fixed coordinate system to the space fixed coordinate system.[44–47] In the present analysis the band constants of $\mathbf{G_3}$ are assumed to be the same as those in $\mathbf{G_1}$ and $\mathbf{G_2}$. The average values of the parameters are also given in Table 1; the calculated spectra by use of the averaged values result as a whole in the less agreement due to a small shift in the peak position.

As discussed previously,[4] $\nu_i$ and $\theta_i$ in Table 1 represent the average value due to various orientations between two oscillators and their distances or various strengths of the H bond. Although it is obvious that $\nu_2$ is due to the normal H-bonded site, $\nu_1$ may result from the $\nu_2$ site perturbed by the OH oscillator in the other chain or the cross-linking of chain, where Y junctions may be included, by inferring that the fraction of Y junctions is 14% in Monte Carlo simulations,[20] which is half of $n_1$ in the present study. Kabeya et al.[19] have reported that lowering temperature reduces the number of Y junctions as well as the non-H-bonded site. This corresponds to the reduction of $n_1$. The Raman spectra suggested above are observed, changing from broad bands with some shoulders at room temperature, as just seen in Figure 2, to two bands at 191 K[29] similar to the spectra in the crystalline state. These support the present assignment of $\nu_1$. Although the Y junction is easily treated in the present approximation, as replacing, for example, $-\nu A(\nu)$ in eq 3 by $-2\nu A(\nu)$, it is not carried out because $\nu_1$ is probably not due to only the Y junction, as noted above.

The values of $\theta_2$ and $\theta_3$ are 71.5 and 72.0°, respectively. In the liquid structure derived from molecular dynamics simulations Torii[6] has reported that the probability of $\theta$ is high in $25 \leq \theta \leq 60°$, although $\theta$ widely ranges in $0 \leq \theta \leq 100°$. On the other hand, Shilov et al.[20] have reported that $\theta$ ranges in ca. $75 < \theta <$ ca. 95°. Hence, $\theta_2$ and $\theta_3$ obtained here are the intermediate of two results and prefer to a tetrahedral packing,[16] although $\theta_1$ prefers to the Torii's result. The wide variation[6,16,20] of $\theta$ as well as the chain length noted later indicates how it is difficult to derive the structure of liquid methanol in the molecular dynamics simulation. It is clear that the quantitative agreements between the observed and simulated spectra are not expected from the analysis based on the incomplete structure derived from the molecular dynamics simulation.[6,7] In Ref. 6 Torii has assumed a unique oscillator for the diagonal element in the eigen value problem, which corresponds to one cluster model of one intrinsic mode in the present approximation. This may be appropriate for analyzing the main peaks in the three types of spectra, in other words, the noncoincidence effect. However, it is clear that one cluster model is insufficient for the present system, as noted above for the shoulder band at ca. 3450 $cm^{-1}$ in the isotropic Raman spectrum. The simulated spectra by Torii give a broad asymmetric band, which results from the many modes with nonzero intensity, where one of the modes in each spectrum has strong intensity, especially in the isotropic Raman spectrum. Although the variable OH stretching force constant related linearly to the distance of the H-bond, O···H, is assumed in Ref. 7, the results are almost the same as those in Ref. 6.

Hence, the present analysis based on the two intrinsic modes differs very much with those by Torii et al.[6–8] In the present approximation some local structures, so-called clusters, are precisely defined, as shown in eq 8, and the remaining parts are self-consistently constructed using the average quantities of the clusters. This means that the coupling among all oscillators in a chain is taken into consideration, as realized from eq 6, which is regarded as a ladder function, as pointed out above. This is the characteristic of the present analysis and the asymmetric shape function of $g_s(\nu)$ and $g_{as}(\nu)$, which is discussed later, reflects the coupling among all oscillators in a chain; the shape function of $g_s(\nu)$ and $g_{as}(\nu)$ in the previous study of the C=O stretching band of acetone is given by the Lorentzian-like band.[4] The present analysis is regarded as a special case of band decomposition by use of the shape function of $\mathbf{G_1}$–$\mathbf{G_3}$. Hence, numerical fitting is necessary to examine adequacy of the present approach. The important thing is the base that $\mathbf{G_1}$–$\mathbf{G_3}$ are inevitable, and it is guaranteed as the result from the two intrinsic modes. There are 22 adjustable parameters, which consist of 13 in Table 1, $n_1$, 6 in $\alpha_i$, and 2 in $\mu_i$. Since two parameters in $\alpha_i$ are reduced from the depolarization ratio in the wide range of the wavenumber and further one or two reduced by assuming the almost axial symmetry of $\alpha_i$, the independent parameters are 18 (19). Although 18 parameters seem to be a large number, they may be adjusted reasonably, by inferring that 18 parameters correspond to the six component bands in the usual band decomposition using the Lorentzians and/or Gaussians, which means two component bands in each infrared or Raman spectrum, whose analysis may be carried out with high reliability, because there are two sets of the noncoincidence effect in the present system, as realized from two intrinsic modes. However, the reliable convergence as obtained here may not be expected from usual analysis using Lorentzians, by referring to the present analysis by use of the more complicated shape functions of $\mathbf{G_1}$–$\mathbf{G_3}$.

Bourderon et al.[27,28] have studied infrared spectra in the overtone region and found four bands at 7135, ca. 6840 or ca. 6630, and 6340 $cm^{-1}$, which are assigned due to monomer,

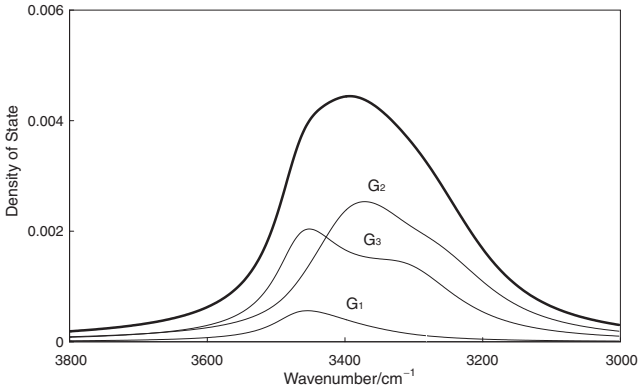


**Figure 3.** The density of state of the OH stretching bands of liquid $CH_3OH$.

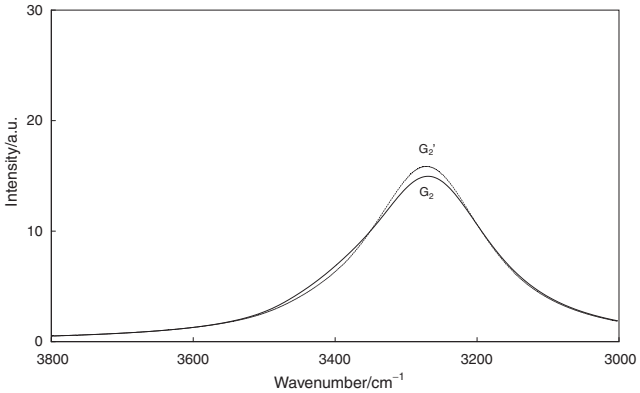


**Figure 4.** The isotropic Raman spectra of the cluster in the chain end, $\mathbf{G_2}'$, and the infinite chain, $\mathbf{G_2}$.

oligomers, and polymers, respectively. On the other hand, they are reasonably assigned to the overtones of the non-H-bonded O–H stretching, the weak band at 3530 $cm^{-1}$ or the shoulder at ca. 3450 $cm^{-1}$, and the main infrared band at 3340 $cm^{-1}$, respectively, in the present study.

The weak band at 3529.2 $cm^{-1}$ may correspond to the band at 3517 $cm^{-1}$ in a dilute methanol solution of $CCl_4$,[37] which is assigned to the H-bonded O–H stretching of an open dimer but not assigned to that in the longer chains. On the other hand, if an OH oscillator is out of the main density of state, the mode appears as a local mode.[42] Figure 3 shows the density of state obtained from the 1,1 and/or 2,2 elements of $\nu\mathbf{G}_i(\nu)$.[23,42] In Figure 3 the density of state with a peak at 3394 $cm^{-1}$ ranges in ca. 3450–ca. 3260 $cm^{-1}$, as realized from the contributions of $\mathbf{G_1}$, $\mathbf{G_2}$, and $\mathbf{G_3}$, and decreases steeply above ca. 3450 $cm^{-1}$. Hence, the 3529.2 $cm^{-1}$ band is far apart from the main density of state and treated as a local mode,[42] by also referring to the small weight of the 3529.2 $cm^{-1}$ band (less than 6%, as shown below). On the other hand, the local mode is not found in some linear chains by ab initio and density functional theory calculations.[37,38] This suggests that the band found here corresponds to a Wallis mode,[48] which is a solitary mode located in a chain end.

The observation of the chain end means finite chains. On the other hand, the other chain end, that is a non-H-bonded OH, is obscure even in the isotropic Raman spectrum. The situation may be similar to the infrared spectrum, by referring that the Raman intensity of the non-H-bonded OH stretching is 1/2.5 smaller than that of the H-bonded one.[49] The intensity of the 3529.2 $cm^{-1}$ band is 5.9% of the whole O–H stretching in the isotropic Raman spectrum. On the other hand, this is only 1.8% in the infrared spectrum, meaning that the intensity of the local mode depends largely on the manner of the observation. The result due to the Raman study may be reliable for expecting the ratio of the chain end, by referring to the smaller change in $\alpha_i$ than $\mu_i$ in the two sites, as described above. Hence, the average molecules in a chain, $\langle N\rangle$, is expected to be ca. 17.

$\langle N\rangle$ evaluated from the molecular dynamics simulations ranges widely as 5–6[14](7),[20] 7–9,[14] 9,[18] 10–12,[16] or 20,[14] depending on the models assumed; it should be noted that the average molecules in an aggregate are to some extent larger than $\langle N\rangle$ because of being Y junctions. Hence, $\langle N\rangle$ evaluated here is somewhat larger than that in the molecular dynamics simulations. This may be due to the evaluation of the Raman tensor, which is assumed to be the same as those in the $\nu_1$ and $\nu_2$ sites. On the other hand, no observation of the non-H-bonded OH band in the isotropic Raman spectrum suggests that $\langle N\rangle$ is considerably large. That is, the ratio of its intensity to the whole one may be given by $\frac{1}{\langle N\rangle}\frac{1}{2.5}$, where the factor 2.5 comes from the intensity of the non-H-bonded OH band.[49] In the case of $\langle N\rangle = 10$ the ratio is ca. 4%, which is comparable with the intensity of the local mode and expected to be observed, as seen in Ref. 7. This suggests $\langle N\rangle > 10$ and the value evaluated here is plausible.

Musso et al.[7] have observed the isotropic and anisotropic Raman spectra in various concentrations of methanol in $CCl_4$. The isotropic and anisotropic Raman peaks shift by ca. 10 and 5 $cm^{-1}$ to the lower wavenumber, respectively, by changing from 1.0 to 0.8 in the mole fraction of methanol. These shifts may correspond to the decrease of the contribution of $\mathbf{G_3}$, as realized from Figure 2. The further dilutions change little the peak positions, although the intensity of the non-H-bonded OH band increases. As reported for the C=O stretching bands of acetone,[4] the main isotropic and anisotropic peaks correspond to the in- and out-of-phase modes of the adjacent oscillators, respectively, which is little affected on $\langle N\rangle$ in accordance with the observations. In quite low concentrations the vibrational spectra have been explained in terms of monomer, open dimer, cyclic trimer, and cyclic tetramer,[37] as noted above, which are, however, completely different with the present result of $\langle N\rangle \approx 17$.

As shown above, the SCBS approximation is applied well to the present system of the finite chain. However, the spectral features of the clusters near the chain end should be examined, because there may be new bands. By referring to eq 6, one of the boundary parameters in the Green's function of the cluster should be replaced by zero, $W_0^2/\sigma$ and so on, depending on the cluster in the chain end, the next site, and so on, respectively. The isotropic Raman spectrum of $\mathbf{G_2}$ in the chain end, $\mathbf{G_2}'$, is compared with $\mathbf{G_2}$ in Figure 4, where $\mathbf{G_2}'$ is drawn in the same manner as $\mathbf{G_3}$ because of the asymmetric matrix of $\mathbf{G_2}'(\nu)$. In $\mathbf{G_2}'$ only the peak appears in near accordance with the peak in $\mathbf{G_2}$, meaning the small change in the spectral feature even in the special case of the chain end. Hence, it is easy to expect quite a small change in the case of $\nu A(\nu) = W_0^2/\sigma$. Since the contribution of the clusters near the chain end to the whole

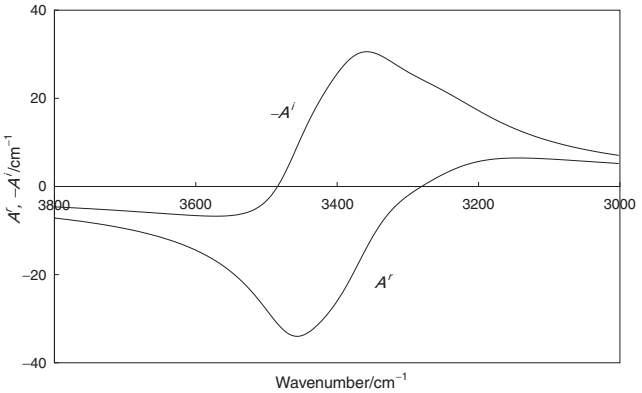


**Figure 5.** The real and imaginary parts of $A(\nu)$, $A^r(\nu)$, and $-A^i(\nu)$.

spectrum is small, it is certain that the present approximation of using the infinite chain is sufficiently high to analyze the vibrational spectra.

It is noted that the line shape of $g_s(\nu)$ is asymmetric with the long wing in the higher wavenumber region, as seen in the isotropic Raman spectrum. This is also true for $g_s(\nu)$ and $g_{as}(\nu)$ in the infrared and depolarized Raman spectra. If $\nu A(\nu)$ in $\mathbf{G_1}$ and $\mathbf{G_2}$ is zero, $g_s(\nu)$ and $g_{as}(\nu)$ are given by the Lorentzian-like band with the peak positions at ca. $\nu_i + \frac{1}{2} f_i^r$ and ca. $\nu_i - \frac{1}{2} f_i^r$, respectively.[4] Hence, the asymmetry of $g_s(\nu)$ and $g_{as}(\nu)$ may result from $\nu A(\nu)$. Figure 5 shows the real and imaginary parts of the boundary parameter $A(\nu)$, $A^r(\nu)$, and $-A^i(\nu)$. $g_s(\nu)$ is given as

$$g_s(\nu) = \frac{1}{{\nu_0}^2 - \nu^2 + i\nu\Gamma_0 - \nu A(\nu) + \nu f} = \frac{1}{{\nu_0}^2 - \nu^2 + i\nu\{\Gamma_0 - A^i(\nu) + f^i\} + \nu\{-A^r(\nu) + f^r\}} \quad (14)$$

This means that the peak position, $\nu_s(\nu)$, and the band width, $\Gamma_s(\nu)$, at $\nu$ are given as: $\nu_s(\nu) \approx \nu_0 + \frac{1}{2}\{-A^r(\nu) + f^r\}$ and $\Gamma_s(\nu) = \Gamma_0 - A^i(\nu) + f^i$, respectively. Since $A^r(\nu)$ is positive with the maximum 6.5 cm$^{-1}$ in $\nu < \nu_0$ ($\nu_0 = \nu_2$ in $\mathbf{G_2}$), the peak position of $g_s(\nu)$ in $\mathbf{G_2}$, $\overline{\nu_s}$, is expected to be ca. $3274.4 - \frac{6.5}{2} = 3271.1$ cm$^{-1}$, which almost coincides with the calculated value at 3270 cm$^{-1}$ in Figure 2a. It is clear that the sharpness below $\overline{\nu_s}$ results from the decrease in $-A^i(\nu)$, as seen in Figure 5, whereas the broadness above $\overline{\nu_s}$ is explained in terms of the changes in $A^r(\nu)$ and $-A^i(\nu)$. Similarly, $\overline{\nu_{as}}$ is approximately expected to be $3365.0 + \frac{34.5}{2} = 3382.3$ cm$^{-1}$, whereas the calculated value is 3377.0 cm$^{-1}$ in $\mathbf{G_2}$ in the infrared spectrum. Since the difference between $\overline{\nu_s}$ and ca. $\nu_0 + \frac{1}{2} f^r$ or $\overline{\nu_{as}}$ and ca. $\nu_0 - \frac{1}{2} f^r$ may correspond to the first moment of $g_s(\nu)$ or $g_{as}(\nu)$, respectively, the asymmetry or the first moment of $g_{as}(\nu)$ is larger than that of $g_s(\nu)$, depending on differences in effective $A^r(\nu)$. It should be noted that $g_{as}(\nu)$ has the long wing below $\bar{\nu}_{as}$; the asymmetric band profile due to the damping coupling is discussed in the recent study.[43] The band width of $g_s(\nu)$ is 225.2 cm$^{-1}$ in $\mathbf{G_2}$ in Figure 2a, which is somewhat smaller than the maximum expected as $\Gamma_2 + f_2^i - \min A^i(\nu) = 232.0$ cm$^{-1}$, where $\min A^i(\nu)$ is $-34.0$ cm$^{-1}$. The band width of $g_{as}(\nu)$ in $\mathbf{G_2}$ is 165 cm$^{-1}$ in the infrared spectrum and considerably larger than the maximum expected from the relation of $\Gamma_2 - f_2^i - \min A^i(\nu) = 146.2$ cm$^{-1}$. This may result from the large change in $A^r(\nu)$ near $\bar{\nu}_{as}$ at 3377.0 cm$^{-1}$.

$\Gamma_i$ in Table 1 includes the contribution of the damping coupling and differs with the band width of the intrinsic mode, $\Gamma_0$, which is, as the first approximation,[4] given by $\Gamma_i - |f^i|$. That is, $\Gamma_0$ for $\nu_2$ is expected to be less than 112 or 134 cm$^{-1}$, which is obtained from $\mathbf{G_2}$ or $\mathbf{G_3}$, respectively, by taking $W_0^i$ into consideration. The large difference in $\Gamma_0$ from $\mathbf{G_2}$ and $\mathbf{G_3}$ indicates that $\Gamma_0$ is not unique in the present assumption that the band constants in $\mathbf{G_3}$ are the same as those in $\mathbf{G_1}$ and $\mathbf{G_2}$, suggesting that $\Gamma_i$ and also $\nu_i$ depend on adjacent oscillators. That is, the new band constants for $\mathbf{G_3}$ may be necessary, which is, however, not treated here, because the present results may give already the new band constant, that is $\Gamma_0 = 112$ and 134 cm$^{-1}$ for $\nu_2$ in $\mathbf{G_2}$ and $\mathbf{G_3}$, respectively, by not taking $W_0^i$ into consideration.

## Summary

A new theoretical approach based on the Green's function is applied to analyze the vibrational spectra of OH stretching bands of $CH_3OH$. The spectra are satisfactorily analyzed on the basis of the three clusters constructed by two intrinsic modes. Two intrinsic modes derived are 3425.5 and 3320.1 cm$^{-1}$, which are assigned to the H-bonded OH stretching perturbed by the OH oscillator in the other chain and the Y junction and that unperturbed, respectively. A weak band found at 3529.2 cm$^{-1}$ is assigned to a local mode in a chain end, by referring to the density of state. The two bands at 3529 and ca. 3450 cm$^{-1}$ are found for the first time as the fundamentals, which make it possible to reassign the overtones without taking short oligomers into consideration. It is realized that $n_1$ decreases with the dilution of methanol in $CCl_4$ and lowering temperature by reference to the observed Raman spectra in Refs. 7 and 29, respectively. The chain structures are clarified in detail from $\theta_2$ and $\theta_3$, which indicate that the configuration about the H bond is the tetrahedral rather than the nearly $sp^2$ configuration evaluated by Torii.[6] It is evaluated that $\langle N \rangle$ is ca. 17 and the effect of the clusters near the chain end on the whole spectrum is small. It is realized that the line shape of $g_s(\nu)$ and $g_{as}(\nu)$ in the symmetric cluster is asymmetric, which is explained in terms of the boundary parameters, $A^r(\nu)$ and $A^i(\nu)$, whose maximum and minimum values relate closely to the peak positions and the bandwidths of $g_s(\nu)$ and $g_{as}(\nu)$, respectively.

## References

1 I. Kanesaka, *Asian J. Spectrosc.* **2001**, *2*, 57.
2 I. Kanesaka, K. Kobayashi, *J. Mol. Struct.* **2005**, *735–736*, 343.
3 I. Kanesaka, K. Kobayashi, *J. Mol. Struct.* **2005**, *753*, 80.
4 K. Kobayashi, I. Kanesaka, *J. Raman Spectrosc.* **2007**, *38*, 436.
5 D. Maillard, C. Perchard, J. P. Perchard, *J. Raman Spectrosc.* **1978**, *7*, 178.
6 H. Torii, *J. Phys. Chem. A* **1999**, *103*, 2843.
7 M. Musso, H. Torii, P. Ottaviani, A. Asenbaum, M. G. Giorgini, *J. Phys. Chem. A* **2002**, *106*, 10152.
8 H. Torii, *Pure Appl. Chem.* **2004**, *76*, 247.
9 D. L. Wertz, R. K. Kruh, *J. Chem. Phys.* **1967**, *47*, 388.

10 A. H. Narten, A. Habenschuss, *J. Chem. Phys.* **1984**, *80*, 3387.
11 D. G. Montague, I. P. Gibson, J. C. Dore, *Mol. Phys.* **1981**, *44*, 1355.
12 Y. Tanaka, N. Ohtomo, K. Arakawa, *Bull. Chem. Soc. Jpn.* **1985**, *58*, 270.
13 W. L. Jorgensen, *J. Am. Chem. Soc.* **1980**, *102*, 543.
14 M. Haughney, M. Ferrario, I. R. McDonald, *J. Phys. Chem.* **1987**, *91*, 4934.
15 M. Matsumoto, K. E. Gubbins, *J. Chem. Phys.* **1990**, *93*, 1981.
16 I. M. Svishchev, P. G. Kusalik, *J. Chem. Phys.* **1994**, *100*, 5165.
17 J. Martí, J. A. Padro, E. Guardia, *J. Mol. Liq.* **1995**, *64*, 1.
18 R. Veldhuizen, S. W. de Leeuw, *J. Chem. Phys.* **1996**, *105*, 2828.
19 T. Kabeya, Y. Tamai, H. Tanaka, *J. Phys. Chem. B* **1998**, *102*, 899.
20 I. Y. Shilov, B. M. Rode, V. A. Durov, *Chem. Phys.* **1999**, *241*, 75.
21 R. Chelli, S. Ciabatti, G. Gardini, R. Righini, P. Procacci, *J. Chem. Phys.* **1999**, *111*, 4218.
22 M. Pieruccini, *J. Phys. Chem. B* **2006**, *110*, 18521.
23 W. H. Butler, *Phys. Rev. B* **1973**, *8*, 4499.
24 U. Liddel, E. D. Becker, *Spectrochim. Acta* **1957**, *10*, 70.
25 L. J. Bellamy, R. J. Pace, *Spectrochim. Acta* **1966**, *22*, 525.
26 H. C. Van Ness, J. Van Winkle, H. H. Richtol, H. B. Hollinger, *J. Phys. Chem.* **1967**, *71*, 1483.
27 C. Bourderon, J.-J. Peron, C. Sandorfy, *J. Phys. Chem.* **1972**, *76*, 869.
28 C. Bourderon, C. Sandorfy, *J. Chem. Phys.* **1973**, *59*, 2527.
29 C. Perchard, J. P. Perchard, *Chem. Phys. Lett.* **1974**, *27*, 445.
30 C. Perchard, J. P. Perchard, *J. Raman Spectrosc.* **1975**, *3*, 277.
31 J. P. Perchard, *Chem. Phys. Lett.* **1976**, *44*, 169.
32 R. Bands, G. Kabisch, K. Pollmer, *J. Mol. Struct.* **1982**, *81*, 35.
33 J. Murto, M. Rasanen, A. Aspiala, E. Kemppinen, *Acta Chem. Scand., Ser. A* **1983**, *37a*, 323.
34 S. Martinez, *Spectrochim. Acta, Part A* **1986**, *42*, 531.
35 A. Sokolowska, Z. Kecki, *J. Raman Spectrosc.* **1993**, *24*, 331.
36 J. E. Bertie, S. L. Zhang, *J. Mol. Struct.* **1997**, *413–414*, 333.
37 J. R. Dixon, W. O. George, M. F. Hossain, R. Lewis, J. M. Price, *J. Chem. Soc., Faraday Trans.* **1997**, *93*, 3611.
38 F. C. Hagemeister, C. J. Gruenloh, T. S. Zwier, *J. Phys. Chem. A* **1998**, *102*, 82.
39 O. Kristiansson, *J. Mol. Struct.* **1999**, *477*, 105.
40 A. Sokolowska, *J. Raman Spectrosc.* **1999**, *30*, 507.
41 E. B. Wilson, Jr., J. C. Decius, P. C. Cross, *Molecular Vibrations*, McGraw-Hill, New York, **1955**.
42 R. J. Elliott, J. A. Krumhansl, P. L. Leath, *Rev. Mod. Phys.* **1974**, *46*, 465.
43 I. Kanesaka, E. Mitsuhashi, *Bull. Chem. Soc. Jpn.* **2008**, *81*, 248.
44 I. Kanesaka, S. Ikeda, *J. Raman Spectrosc.* **1992**, *23*, 181.
45 I. Kanesaka, T. Matsuda, T. Niwa, *J. Raman Spectrosc.* **1994**, *25*, 245.
46 I. Kanesaka, T. Matsuda, Y. Morioka, *J. Raman Spectrosc.* **1995**, *26*, 239.
47 I. Kanesaka, *Asian J. Spectrosc.* **1998**, *2*, 44.
48 R. F. Wallis, *Phys. Rev.* **1957**, *105*, 540.
49 N. Abe, M. Ito, *J. Raman Spectrosc.* **1978**, *7*, 161.